Adjoint Sensitivity of FARMS to the Forecasting Variables of WRF-Solar

Preprint

Jaemo Yang,[1] Manajit Sengupta,[1] Yu Xie,[1]
Pedro A. Jimenez,[2] and Ju-Hye Kim[2]

[1] National Renewable Energy Laboratory
[2] National Center for Atmospheric Research

NREL is a national laboratory of the U.S. Department of Energy
Office of Energy Efficiency & Renewable Energy
Operated by the Alliance for Sustainable Energy, LLC

This report is available at no cost from the National Renewable Energy Laboratory (NREL) at www.nrel.gov/publications.

Adjoint Sensitivity of FARMS to the Forecasting Variables of WRF-Solar

Preprint

Jaemo Yang,[1] Manajit Sengupta,[1] Yu Xie,[1]
Pedro A. Jimenez,[2] and Ju-Hye Kim[2]

[1] National Renewable Energy Laboratory
[2] National Center for Atmospheric Research

NOTICE

ADJOINT SENSITIVITY OF FARMS TO THE FORECASTING VARIABLES OF WRF-SOLAR

Jaemo Yang[1], Manajit Sengupta[1], Yu Xie[1], Pedro A. Jimenez[2], Ju-Hye Kim[2]
[1]National Renewable Energy Laboratory, Golden, CO, USA
[2]National Center for Atmospheric Research, Boulder, CO, USA

ABSTRACT: This study presents the development and application of an adjoint model for investigating the sensitivity of solar radiation to forecasted variables from Weather Research and Forecasting-Solar (WRF-Solar). The first part of this study focuses on developing an adjoint model for the Fast All-sky Model for Solar Applications (FARMS) to investigate the input variables having the highest sensitivity to global horizontal irradiance, direct normal irradiance, and diffuse horizontal irradiance, which are the output variables. The applicability and usefulness of the adjoint sensitivity approach are demonstrated by conducting a sensitivity analysis under various scenarios defined by low, medium, and high values for the input variables. This preliminary study uses elasticity values to understand the sensitivity of solar radiation to the input variables (e.g., solar zenith angle, Ångström turbidity coefficient, and cloud optical depth) of FARMS. This presentation will illustrate the implemented methodology and the obtained sensitivity results for FARMS as well as future research steps that will lead to the development of high-quality probabilistic solar forecasts.

Keywords: WRF-Solar, Sensitivity analysis, FARMS, Adjoint/Tangent linear model

1 INTRODUCTION

The contribution of solar energy to the electric grid has been rapidly increasing during the last few years, and integration has become a major source of concern for system operators. A key challenge in integrating solar generation is accurately predicting the confidence in a forecast of solar power. This can be achieved by creating an ensemble of forecasts through the optimized perturbation of initial conditions and generating a probabilistic forecast using the ensemble members.

For solar forecasting technologies, the Weather Research and Forecasting-Solar (WRF-Solar) model [1] was developed by the National Center for Atmospheric Research and its partners to better model the processes that impact solar irradiance on the ground. WRF-Solar is the only publicly available model worldwide that has been developed to provide accurate solar forecasts through significant improvements in the representation of aerosols, cloud formation, and radiative transfer calculations compared to the baseline WRF model.

WRF-Solar can now form the basis for developing probabilistic forecasts for the solar energy community. Prior to developing the probabilistic solar prediction using WRF-Solar, we need to identify the WRF-Solar modules that directly impact cloud formation and dissipation and develop an adjoint model (ADM) [2] of the target module. This enables an estimation of the sensitivity of the model output with respect to inputs without requiring thousands of runs to perturb each input individually. The comprehensive analysis from the adjoint modeling effort will contribute to optimizing the ensemble prediction through a down-selection of variables that are relevant for the WRF-Solar ensemble.

In this study, we built an ADM for the Fast All-sky Radiation Model for Solar Applications (FARMS) [3], which is one component of WRF-Solar for calculating global horizontal irradiance (GHI), direct normal irradiance (DNI), and diffuse horizontal irradiance (DHI). We then analyzed the sensitivity of FARMS to the forecasting variables under various scenarios.

2 METHODOLOGY

2.1 Theory of Adjoint

The ADM is derived from the tangent linear model (TLM), which is derived from the forward model (FWM). The FWM is defined as follows:

$$\mathbf{Y} = M(\mathbf{X}) \tag{1}$$

where M is the nonlinear model, $\mathbf{X}$ is the matrix of the input variables of model M, and $\mathbf{Y}$ is the column vector of the output variables of model M. The tangent linear operator ($\mathbf{L}$), which gives the derivates of the FWM (1) with respect to the independent varaibles, is given as:

$$\mathbf{L} = \frac{\partial \mathbf{Y}}{\partial \mathbf{X}} \tag{2}$$

The TLM of (1) can be expressed as:

$$d\mathbf{Y} = \mathbf{L}d\mathbf{X} \tag{3}$$

where $d\mathbf{X}$ and $d\mathbf{Y}$ are the input and output of the TLM (3). If $\langle \ , \ \rangle$ is a scalar product and $\mathbf{A}$ is a linear operator, the adjoint of $\mathbf{A}$ can be mathematically defined as the operator of $\mathbf{A^T}$ statisfying:

$$\langle \mathbf{AX}, \mathbf{Y} \rangle = \langle \mathbf{X}, \mathbf{A^T Y} \rangle \tag{4}$$

For the sensitivity study, any differentiable function, $R(\mathbf{Y})$, can be used to define a response function comprising output variable $\mathbf{Y}$. Changes in the state of the model output entail changes to the value of a response function:

$$dR = \langle \frac{\partial R}{\partial \mathbf{Y}}, d\mathbf{Y} \rangle = \langle \frac{\partial R}{\partial \mathbf{Y}}, \mathbf{L}d\mathbf{X} \rangle = \langle \mathbf{L^T} \frac{\partial R}{\partial \mathbf{Y}}, d\mathbf{X} \rangle \tag{5}$$

If we use the definition of the differential for input variable $\mathbf{X}$ and response function R:

$$dR = \left\langle \frac{\partial R}{\partial \mathbf{X}}, d\mathbf{X} \right\rangle \qquad (6)$$

Finally, the relationship between the input and output variables for the response function R can be expressed as:

$$\frac{\partial R}{\partial \mathbf{X}} = \mathbf{L}^{\mathbf{T}} \frac{\partial R}{\partial \mathbf{Y}} \qquad (7)$$

In (7), the output of the ADM is the gradient of a response function R with respect to the model input. In this study, the GHI, DNI, and DHI are used as the response function instead of any errors or averaged forecasts; therfore, the d(GHI), d(DNI), and d(DHI) are analyzed with respect to the input variables for FARMS.

2.2 The Transformation of Algorithms in Fortran

The Transformation of Algorithms in Fortran (TAF) [4], [5] is a tool for automatic differentiation. TAF is a source-to-source transformation tool for functions written in Fortran-90/95 or FORTRAN-77. The TAF software package enables a sensitivity analysis of complex functions that have been coded into Fortran. TAF generates an adjoint code of forward models that evaluates the derivative of the output variables with respect to the input variables, thereby providing the capability to analyze the sensitivity of the input variables to the output. For this study, TAF is used to produce the adjoint code of FARMS and analyze the sensitivity of the input variables to the output variables, which are related to solar radiation.

2.3 Validation of Tangent Linear and Adjoint Codes

The validation of the ADM and TLM should be strictly verified after the the AD and TL codes are built by TAF. A consistency of TLM with its FWM needs to be verified with a linearity test fisrt because the ADM is a concomitant of the TLM. Then the accuracy of the ADM is checked by an adjointness test verifying a consitency of ADM with TLM.

The linearity test compares the ratio of the derivative of the forecast variables with respect to the model state variables in the FWM and the solutions from TLM [6], [7]. (8) is used for correctness check for TLM. The ratio will be 1 if the tangent linear code is correctly developed.

$$\Phi(\lambda) = \frac{\|f(\mathbf{x} + \lambda g\_x) - f(\mathbf{x}))\|}{\|g\_f(\mathbf{x}, \lambda\, g\_x)\|}, \lim_{\lambda \to 0} \Phi(\lambda) = 1 \qquad (8)$$

In (x), the $f(\mathbf{x})$, $g\_f(\mathbf{x}, g\_x)$, and $a\_f(\mathbf{x}, a\_x)$ denote an FWM, a TLM, and an ADM, respectively, where $\mathbf{x}$, g_x, and a_x are the column vectors of the model-state variables, perturbations of the state variables, and the adjoint of the state variables, respectively.

Using the adjointness relationship, the correctness of the adjoint code was tested by:

$$\langle g\_f(\mathbf{x}, g\_x), g\_f(\mathbf{x}, g\_x) \rangle \qquad (9)$$
$$= \langle a\_f[\mathbf{x}, g\_f(\mathbf{x}, g\_x)], g\_x \rangle$$

In FARMS, 13 input variables—including surface pressure, surface albedo, asymmetry factor of aerosol, solar zenith angle, aerosol optical depth, Ångström wavelength exponent, total precipitable water, cloud optical depth, and cloud effective radius—are used to implement the linearity and adjointness tests. First, the linearity test is performend for each FARMS input variable with sequentially reduced perturbations. Figure 1 shows the results of the linearity (6 input variables) and adjointness tests for FARMS. The results show that the FARMS TLM approximates well the derivative of the FWM solution because the TLM solutions are going to 1 as the perturbations decreased and approach zero. In addition, when we perturb all 13 variables at once, the FARMS TLM approximates well the derivative of the nonlinear model solution, which means that the tangent linear code was correctly developed by the TAF. In the adjointess test results, the numbers of the left-hand side and right-hand side are exactly the same within a machine precision accuracy. This indicates that an AD code was developed correctly with the TL code.

```
1. Linearity test

         perturbation                    p_pa                   albdo
   0.1000000000000000      0.99999982364046653      1.01886477327702811
   0.0100000000000000      0.99999998236404184      1.00181589165434327
   0.0010000000000000      0.99999999823640414      1.00018093007685141
   0.0001000000000000      0.99999999982364041      1.00001808646025850
   0.0000100000000000      0.99999999998236404      1.00000180858059473
   0.0000010000000000      0.99999999999823640      1.00000018085740521
   0.0000001000000000      0.99999999999982364      1.00000001808573398
   0.0000000100000000      0.99999999999998236      1.00000000180857333
   0.0000000010000000      0.99999999999999824      1.00000000018085733
   0.0000000001000000      0.99999999999999982      1.00000000001808573
   0.0000000000100000      1.00000000000000000      1.00000000000180857
   0.0000000000010000      1.00000000000000026      1.00000000000018086

         perturbation                    alpha                       w
   0.1000000000000000      1.01297889692556379      0.99833807655010926
   0.0100000000000000      1.00128749954634479      0.99983346520669115
   0.0010000000000000      1.00012864664708110      0.99998334308727627
   0.0001000000000000      1.00001286363222186      0.99999833427438476
   0.0000100000000000      1.00000128635289504      0.99999983342709504
   0.0000010000000000      1.00000012863518336      0.99999998334270607
   0.0000001000000000      1.00000001286351440      0.99999999833427057
   0.0000000100000000      1.00000000128634852      0.99999999983342706
   0.0000000010000000      1.00000000012863195      0.99999999998334271
   0.0000000001000000      1.00000000001286029      0.99999999999833427
   0.0000000000100000      1.00000000000128312      0.99999999999983343
   0.0000000000010000      1.00000000000012541      0.99999999999998334

         perturbation                 re_qcloud                 re_qice
   0.1000000000000000      0.00054592688511941      0.00041763418180853
   0.0100000000000000      0.00545926885119413      0.00417634181808530
   0.0010000000000000      0.05459268851194133      0.04176341818085303
   0.0001000000000000      0.54592688511941326      0.41763418180853029
   0.0000100000000000      0.99448710487399171      1.05846382261075610
   0.0000010000000000      0.99944518110118040      1.00569555430513386
   0.0000001000000000      0.99994448253666235      1.00056808533263866
   0.0000000100000000      0.99999444789698367      1.00005679386952391
   0.0000000010000000      0.99999944478613725      1.00000567924035214
   0.0000000001000000      0.99999994447857811      1.00000056792256925
   0.0000000000100000      0.99999999444785746      1.00000056792244227
   0.0000000000010000      0.99999999944478574      1.00000000567922408

2. Adjointness test

   Val_TL   177428010441.85327915938944692656
   Val_AD   177428010441.85327915938944692656
```

Figure 1. Results of tangent linear and adjointness tests for the FARMS module.

2.4 Scenario Analysis

The sensitivity study is implemented by using various FARMS scenarios representing clear-sky and cloudy-sky conditions. The adjoint version of the FARMS code is developed first. Next, reasonable values representing the three levels (low, medium, and high) are assigned to the

2

input variables. Table 1 lists the physical inputs of FARMS and the conditions for clear skies and cloudy skies (water/ice cloud). For clear-sky conditions, the surface pressure, albedo, asymmetry factor of aerosol, cosine value of solar zenith angle (referred to as cosz), Ångström turbidity coefficient, and precipitable water vapor are adjusted for the three levels indicating low-medium-high values. For cloudy conditions, the input variables are surface pressure, albedo, cosine value of solar zenith angle, precipitable water vapor, cloud optical depth, and cloud effective radius. The leveled input values for the clear- and cloudy-sky conditions are also presented in Table 1. Last, the FARMS adjoint code is run for 729 cases with the three levels (low, medium, high), and individual scenarios that contain 243 cases are analyzed (i.e., all cases when albedo is high) (see Fig. 2).

2.5 Elasticity for Scaling in Analysis of Sensitivity

One challenge in analyzing sensitivities is that independent variables of the models have different units. Especially for the comparisons of sensitivities for various input variables, the interpretation of the sensitivity results is complicated by issue of scale. Therefore, elasticity [8] is a reasonable method to estimate the effect of a proportional change in output variable related to a rate of proportional change in input variable. The elasticity is defined as follows: where x and y are input and output variables, respectively. The elasticity, which is dimensionless, is used to estimate the sensitivity of the output variables with respect to the input variables for FARMS. For example, if the elasticity of the albedo is 0.5 for DHI, this means that a 1% increase in albedo will cause a 0.5% increase in DHI.

Table 1. FARMS input variables and conditions for clear and cloudy skies. The three levels are low (L), medium (M), and high (H).

Input variable	Clear sky	Cloudy sky	
		Water cloud	Ice cloud
Surface pressure (Pa)	L: 98000 M: 101300 H: 108000	L: 98000 M: 101300 H: 108000	L: 98000 M: 101300 H: 108000
Albedo	L: 0.2 M: 0.5 H: 0.8	L: 0.2 M: 0.5 H: 0.8	L: 0.2 M: 0.5 H: 0.8
Asymmetry factor of aerosol	L: 0.7 M: 0.8 H: 0.95	0	0
Solarangle (cosz, radian)	L: 0.2 M: 0.6 H: 0.9	L: 0.2 M: 0.6 H: 0.9	L: 0.2 M: 0.6 H: 0.9
Ångström turbidity coefficient	L: 0.1 M: 0.3 H: 0.6	0	0
Ångström wavelength exponent	1	0	0
Precipitable water vapor (mm)	L: 5 M: 10 H: 30	L: 5 M: 10 H: 30	L: 5 M: 10 H: 30
Cloud optical depth for vapor	0	L: 0.5 M: 3.0 H: 10.0	0
Cloud optical depth for ice	0	0	L: 0.5 M: 3.0 H: 10.0
Cloud optical depth for snow	0	0	0
Cloud effective radius for vapor (m)	0	L: 5.00E-06 M: 1.50E-05 H: 3.00E-05	0
Cloud effective radius for ice (m)	0	0	L: 1.00E-05 M: 3.00E-05 H: 6.00E-05
Cloud effective radius for snow (m)	0	0	0
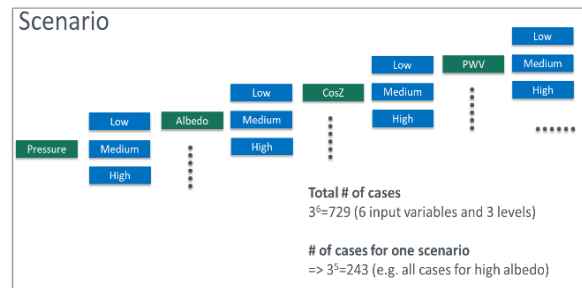
Figure 2. Schematic showing the scenarios with low, medium, and high levels for the input variables.

$$\text{Elasticity} = \frac{x}{y} \times \frac{\partial y}{\partial x} \qquad (10)$$

3   RESULTS

For FARMS, the sensitivities of the input variables to the output variables are analyzed with elasticity values. Again, the input variables are surface pressure, albedo, asymmetry factor of aerosol (clear sky), cosz, Ångström turbidity coefficient (clear sky), precipitable water vapor, cloud optical depth (cloudy sky), and cloud effective radius (cloudy sky); and the output variables are GHI, DNI, and DHI. The elasticity values are calculated for all 243 cases for one scenario.

Figure 3 shows an example of the variation of elasticity for GHI under clear-sky conditions with respect to the Ångström turbidity coefficient (referred to as beta). Most elasticity values are negative because physically beta influences the extinction of the solar radiation reaching the surface under clear-sky conditions. In Fig. 3, GHI is more sensitive to beta when the asymmetry factor of aerosol is low compared to the medium-high scenarios of the asymmetry factor of aerosol. Also, beta shows an increase in the sensitivity range in scenarios of cosz when the value of cosz increases. Under all conditions of low-medium-high surface pressure and precipitable water vapor, beta exhibits similar and consistent elasticity characteristics (i.e., almost identical sensitivities).

Figure 4 exhibits an average of elasticity calculated over 243 cases for each input variable and each scenario (clear-sky condition). As expected, cosz shows the largest elasticity value for GHI, DNI, and DHI under all scenarios. In clear-

3

sky conditions, the beta is very sensitive to DNI because atmospheric turbidity mainly causes attenuation of solar radiation that reaches the surface.
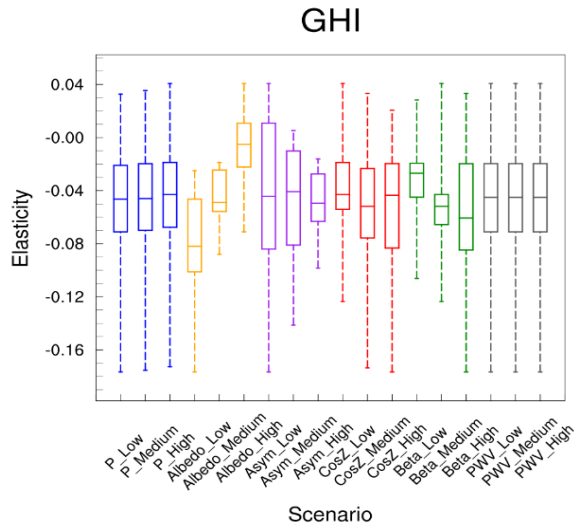
Figure 3. Elasticity (scaled sensitivity) of GHI with respect to Ångström turbidity coefficient for each scenario. Each box-whisker plot includes 243 elasticity values, calculated for individual scenarios (bar: median, box: interquartile range, whiskers: range, and error bars: minimum and maximum).
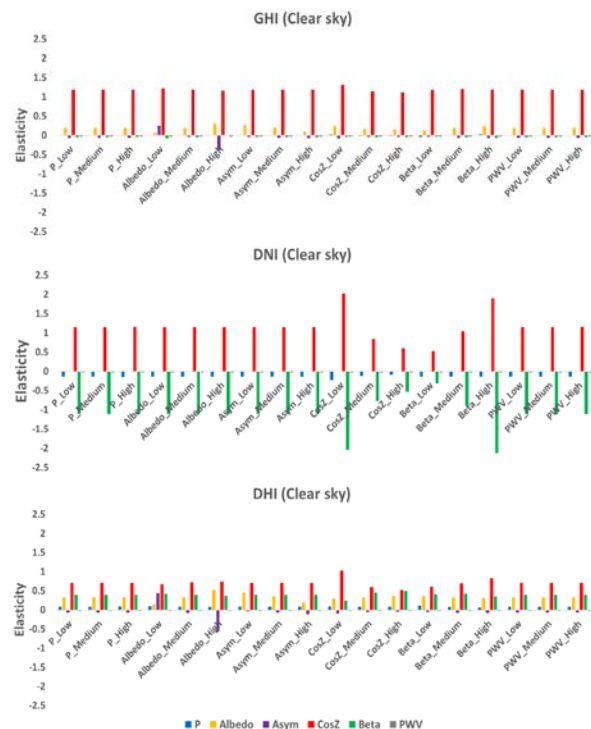
Figure 4. Average of elasticity calculated over 243 cases for each input variable and each scenario. Note that this figure shows the results of GHI, DNI, and DHI for the clear-sky condition.
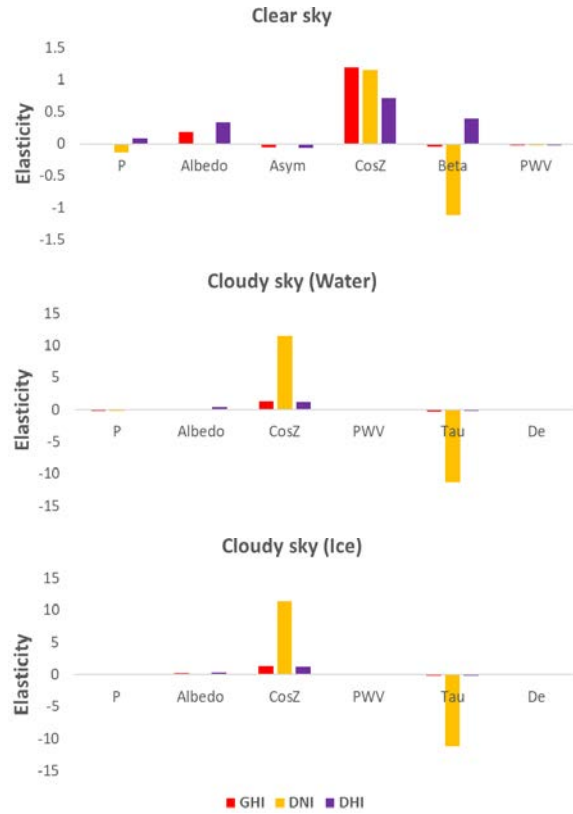
Figure 5. Average of elasticity for GHI, DNI, and DHI calculated over all scenarios for each input variable.

The input variables that demonstrate the highest sensitivities for the output variables for FARMS are identified in Fig. 5. Figure 5 shows an averaged elasticity for all scenarios for GHI, DNI, and DHI for the clear-/cloudy-sky conditions. With the exception of cosz, the albedo and beta exhibit the highest sensitivities for GHI and DNI individually under clear-sky conditions. For DHI under the same conditions, the sensitivity and elasticity of the albedo and beta are almost identical and comparable to cosz. Under cloudy-sky conditions, the results of the output variables of FARMS are very similar for water and ice clouds. The notable sensitivities of cosz and tau (cloud optical depth) for DNI are attributed to the transmittance of the cloud for direct incident radiation and scattering by the cloud for direct outgoing radiation, which are mainly governed by cosz and tau. For GHI and DHI, the tau and albedo are more sensitive compared to the other input variables, with the exception for cosz.

4   SUMMARY

In this work, we presented a sensitivity analysis framework for WRF-Solar modules that will subsequently be used to determine the set of input variables that have the highest impact on the accuracy of the prediction of solar radiation. The sensitivity analysis that enables the selection of ensemble members for probabilistic solar forecasting is based on adjoint modeling. As an initial step toward developing the framework for probabilistic forecasts using an ensemble based WRF-Solar, FARMS is selected, and the

4

adjoint model of FARMS is developed to identify the input variables with lower/higher order sensitivities. In addition, the sensitivity analysis is conducted using various scenarios that include low, medium, and high levels of input variables for FARMS. The method developed in this study will be used to optimize WRF-Solar ensembles so that this model can be used operationally for solar forecasting for grid operations.

REFERENCES

[1] Jimenez, P.A., J. P. Hacker, J. Dudhia, S. E. Haupt, J. A. Ruiz-Arias, C. A. Gueymard, G. Thompson, T. Eidhammer and A. Deng, 2016: WRF-Solar: Description and Clear-Sky Assessment of an Augmented NWP Model for Solar Power Prediction. Bulletin of the American Meteorological Society, 97, 1249-1264.
[2] Errico, R., 1997: What Is an Adjoint Model?. Bulletin of the American Meteorological Society, 78, 2577–2591.
[3] Xie, Y., Sengupta, M., Dudhia, J., 2016: A Fast All-sky Radiation Model for Solar applications (FARMS): Algorithm and performance evaluation. Solar Energy., 135, 435-445.
[4] Giering, R. and Kaminski, T., 2003: Applying TAF to generate efficient derivative code of Fortran 77-95 programs. PAMM, 2(1), 54-57.
[5] Giering, R., T. Kaminski, and T. Slawig., 2005: Generating Efficient Derivative Code with TAF: Adjoint and Tangent Linear Euler Flow Around an Airfoil. Future Generation Computer Systems, 21(8), 1345-1355.
[6] Xiao, Q., and Coauthors., 2008: Application of an Adiabatic WRF Adjoint to the Investigation of the May 2004 McMurdo, Antarctica, Severe Wind Event. Monthly Weather Review, 136, 3696-3713.
[7] Zhang, X., Huang, X.-Y., and Pan, N., 2013: Development of the Upgraded Tangent Linear and Adjoint of the Weather Research and Forecasting (WRF) Model. Journal of Atmospheric and Oceanic Technology, 30, 1180-1188.
[8] Link, W. A., and Doherty, P. F., 2002: Scaling in Sensitivity Analysis. Ecology, 83(12), 3299–3305.